Designing the Method for Optical In Vitro Monitoring of the Cell-Mediated Scaffold Technology for Bone Regeneration Based on Laser-Induced Fluorescence Spectroscopy

Abstract. One of the main unsolved problems in traumatology and orthopedics is reconstruction of critical-sized segmental bone defects. We believe that implementation of noninvasive monitoring of the bioengineering stages for cell-mediated bone scaffold by laser-induced fluorescence (LIF) can become a positive aspect in mastering this technique. An electrospun scaffold model (parameters: 10 wt. % polycaprolactone; 5% wt type A gelatin; mean fiber diameter 877.1 ± 169.1, and contact angle 45.3°) seeded with BHK IR cell culture (182 ± 38 cells/mm²) was used to show the principal possibility of differentiating between the scaffold seeded and unseeded with cells. First of all, the fluorescence spectra of the cell-seeded scaffold contain a peak at 305 nm for the excitation range of 230–290 nm, which can be used to differentiate between the samples. An increase in fluorescence intensity of the cell-seeded scaffold in the range of 400–580 nm upon excitation at 230–340 nm is also noticeable. The wavelength of 250 nm is characterized by high signal intensity and is most suitable for differentiation between the samples.

INTRODUCTION

One of the main unsolved problems in traumatology and orthopedics is reconstruction of critical-sized segmental bone defects. The current standard in treatment of these defects is the medical technologies that use auto-bone grafts, which may involve pain and risk of trauma for patients. The use of various allogenic and xenogenic osteoplastic materials is associated with a number of surgical, biological, and ethical limitations [1–3].

An alternative approach is fabrication of tissue-engineered bone equivalents using the patient's own cells. The basic approaches to fabrication of tissue-engineered equivalents are well-known and include biocompatibility and osteoinductivity of materials, the possibility to ensure reliable fixation, insertion of biomimetic elements in the construct, nontoxicity, predetermined bioresorption, the use of growth factors and progressive cell culture techniques [3, 4].

A recent review has demonstrated that the trend of cellular component of scaffold for bone regeneration has changed from osteoprogenitor cells to endothelial progenitor cells. Preimplantation vascularization of scaffolds is the key element of successful bone regeneration when using scaffold-mediated technologies [5]. Another direction that has recently been launched in bioengineering of cell-mediated bone scaffolds for bone regeneration is

cultivation in bioreactors, where the mechanotransduction effects on cells are analyzed (in particular, enhanced osteogenic differentiation of mesenchymal stem cells with increased mineralization of bone matrix) [6]. The variants of using the integrated approach to scaffold biotechnology upon cultivation in a bioreactor are also being discussed. Despite the enhanced osteogenic differentiation when coculturing mesenchymal stem cells and endothelial progenitors, no vascular network formation has been observed by day 7 when culturing scaffolds in a bioreactor. Meanwhile, subsequent investigation of the scaffolds precultured in a reactor using the subcutaneous model showed enhanced cell chimerism and early formation of the vascular network [7].

According to the analytical review, a number of reasons impede clinical application of pre-vascularized scaffolds aimed at reconstructing the critical-size bone defects: poor vascularization, insufficient mechanical stability, poorly studied osteointegration capacity of bioresorbable scaffolds, and the risk of infection [8].

We hypothesized that designing the method of noninvasive monitoring the scaffold state after it has been seeded with target cells can largely determine the fate of cell-mediated scaffold technologies. Laser-induced fluorescence (LIF) spectroscopy was suggested as a candidate. This method has previously been used in a series of studies to prove the possibility of determining the degree of mineralization of heart and vessel valves, to assess myocardial viability, and to monitor the stages of decellularization of heart valve grafts [9–11].

This study was aimed at considering the possibility of designing the method for diagnosing the state of cell scaffold to replace bone defects based on laser-induced fluorescence spectroscopy.

MATERIAL AND METHODS

The scaffold sheet was formed on an NF-103 electrospinning machine (MECCO, Japan) at different process parameters. The following materials were used to fabricate the sheet: polycaprolactone (80 kDa, Sigma Aldrich), gelatin (type A, Sigma Aldrich). 1,1,1,3,3,3-Hexafluoropropanol (Sigma Aldrich), acetone (Reakhim, chemical purity grade), and glacial acetic acid were used as solvents.

The scaffold sheet was assessed using an LSM 710 laser scanning microscope (Carl Zeiss, Germany) with excitation at 405 nm and simultaneous detection of passing light. Fiber morphometry was carried out, and the defects were detected. After gold sputtering (TESCAN, Czech Republic), a study was carried out using a MIRA3 electron scanning microscope. The hydrophilicity of the materials used to form cell matrices was assessed by determining the contact angle.

The characteristics of the resulting scaffold sheet were as follows: composition—10 wt. % polycaprolactone and 5 wt. % gelatin, mean fiber diameter 877.1 ± 169.1 , contact angle 45.3° . Cold sterilization with ethylene oxide was performed at 36° C.

Cell culture: The sheet was placed at the bottom of 6-well plates (TPP, Switzerland). 1.5 mL of DMEM medium (Gibco, USA) containing 10% of fetal bovine serum (HyClone, USA) and a penicillin (100 U/mL)–streptomycin (100 μ g/mL) mixture were added. 100,000 BHK IR cells were added to the wells containing the sheet under study. The adhesion and cytotoxicity was analyzed using an 18-hour MTT assay. The average cell-seeding density was 182 ± 38 cells/mm²; MTT assay showed no more than 1.1% of toxically damaged cells. The samples seeded with BHK IR cells were then studied by LIF.

We used a spectroscopic measuring setup shown in Fig. 1 to investigate laser-induced fluorescence of the samples. Samples were irradiated using a Vibrant HE 355 II +UV pulse-periodic laser (Opotek, USA) equipped with an optical parametric oscillator (OPO) that provides tuned laser radiation with pulse energy up to 3 mJ within the range of 210–355 nm. A laser beam passed through the external filtration system consisting of a reflector telescope with the diaphragm coinciding with the focal point of the mirrors in order to attenuate radiation for double wavelength generation scattered inside the OPO system. The laser pulse energy was varied appreciably strongly from pulse to pulse. To monitor the energy, some radiation (~5%) was diverted to the reference sensor using a semi-transparent UV-1 quartz plate to be subsequently normalized. The sensor consisted of an FD-24 photodiode with the truncated glass inlet window, matte plate installed in front of the photodiode to reduce the effect of beam heterogeneity on measurements, an integrating capacitor, and a repeater on the operational amplifier. The signal generated by the sensor was measured by the L-783 analog-to-digital converter (L-card, Russia) installed in the process computer.

The laser beam was then directed at the analyzed sample whose fluorescence was fed into the spectrometer using a spherical reflector. A spectrometer based on an Action SP2300 spectrograph (Princeton Instruments, USA) equipped with a diffraction grating and a cooled Pixis 256 CCD matrix with open electrodes (Princeton Instruments, USA) were used to record fluorescence.

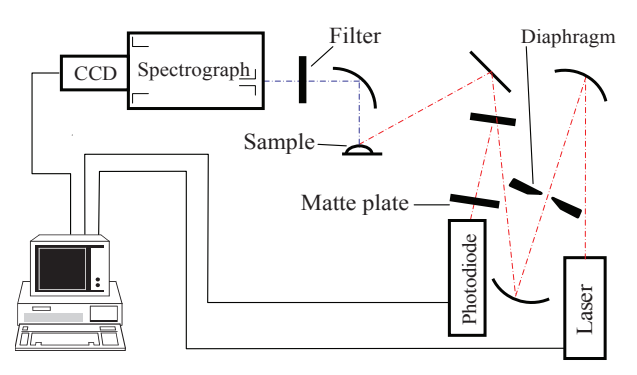


FIGURE 1. Block-diagram of the measuring setup for LIF spectroscopy

The inlet slit of the spectrometer coincided with the focal point of the reflector, so we measured the signal averaged over the sample surface. In order to protect the spectrometer matrix against being damaged by scattered laser radiation, we placed neutral filters with the UV border determined by the wavelength of laser radiation in front of the inlet slit of the spectrometer. The measurements within the laser wavelength range of 210–290 nm were carried out using a colorless polymer filter with the short-wave border beyond 300 nm; measurements at 300–340 nm were carried out using a BS-8 filter (border 400 nm). Different fluorescence spectra were recorded by varying the laser radiation wavelength in the range between 210 and 340 nm. These 2D data arrays are known as the excitation–emission matrices.

RESULTS AND DISCUSSION

Fluorescence excitation-emission matrices were recorded for the scaffold sheet (Fig. 2), suspension of BHK IR cells (Fig. 3), DMEM cell medium (Fig. 4), and the cell-seeded scaffold sheet (Fig. 5). Prior to analysis, the cell-seeded sheet was washed in a physiological solution.

The scaffold sheet matrix (Fig. 2) is complex-shaped and contains many fluorescence maxima; the spectra depend on excitation wavelength. In this connection, it is impossible to determine the main number of fluorescent components in it. The fluorescence spectra of cell suspension (Fig. 3) and cell medium (Fig. 4) also depend on excitation wavelength, while the fluorescence maximum at 330 nm is caused by high concentration of tryptophan fluorophore. The excitation-emission matrix of cell suspension is probably largely determined by the presence of culture medium: the fluorescence spectra virtually coincide with one another, although the excitation spectra differ rather significantly in the shortwave region. The fluorescence spectrum of the cell-seeded scaffold sheet contains a pronounced maximum at 305 and a shoulder at 400–580 nm.

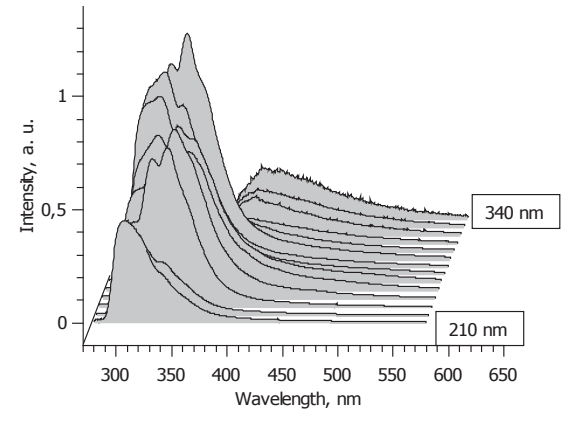


FIGURE 2. The normalized excitation-emission matrix of the scaffold sheet

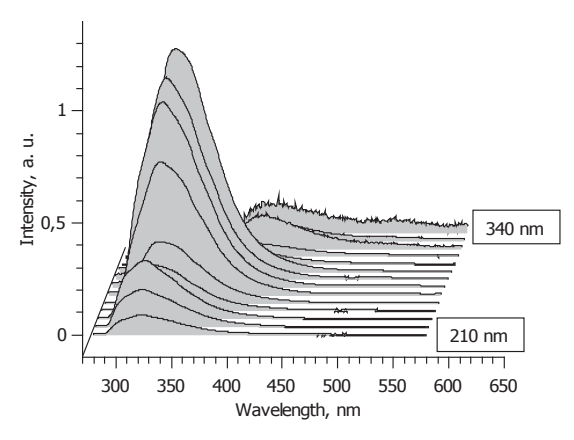


FIGURE 3. The normalized excitation-emission matrix of BHK IR780 cell suspension

To search for diagnostic criteria, one can compare the resulting matrices, in terms of excitation of fluorescence features. It is most convenient to compare the shapes of fluorescence spectra recorded at a certain optimal excitation wavelength. For each excitation wavelength within the range from 210 to 340 nm, we compared the fluorescence spectra of the scaffold sheet, BHK IR cell suspension, and the cell-seeded sheet normalized to the intensity maximum. At excitation wavelength within the range from 230 to 290 nm, the fluorescence spectra of the cell-seeded sheet have a clearly pronounced maximum at 305 nm compared to those of the unseeded sheet and cell suspension. Furthermore, the spectrum of the cell-seeded sheet is characterized by increased fluorescence intensity within 400–580 nm at the same excitation wavelengths. Figure 6 compares the fluorescence spectra at excitation wavelength of 250 nm, which most clearly illustrates the afore-described differences in the spectra. An increase in fluorescence intensity of the cell-seeded sheet at 400–580 nm is also clearly seen for excitation wavelengths of 300–340 nm. The spectra of samples for the excitation wavelength of 330 nm are compared in Fig. 7.

CONCLUSION

Generally speaking, differentiation can be made between the scaffold sheets either seeded or unseeded with BHK IR cells using LIF spectroscopy based on the data on fluorescence spectra of the samples for different excitation wavelengths. First of all, the fluorescence spectra of the cell-seeded scaffold sheet for the excitation range of 230–290 nm contains a peak at 305 nm, which can be used to differentiate between the samples. There is also a noticeable increase in fluorescence intensity of the seeded scaffold sheet at 400–580 nm under excitation at wavelength of 230–340 nm. The wavelength of 250 nm can be considered to be most suitable for differentiation; it is characterized by high signal intensity and the most noticeable differences between various types of samples.

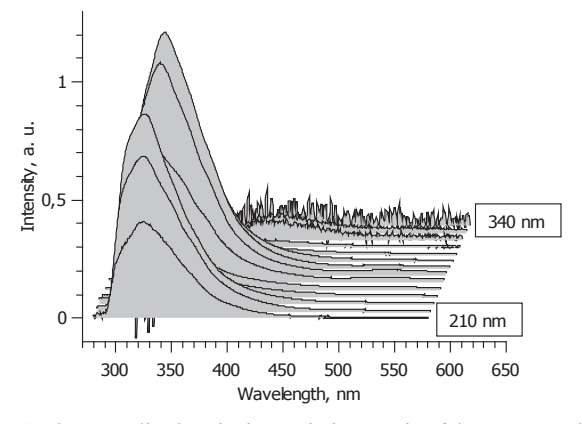


FIGURE 4. The normalized excitation-emission matrix of the DMEM cell culture

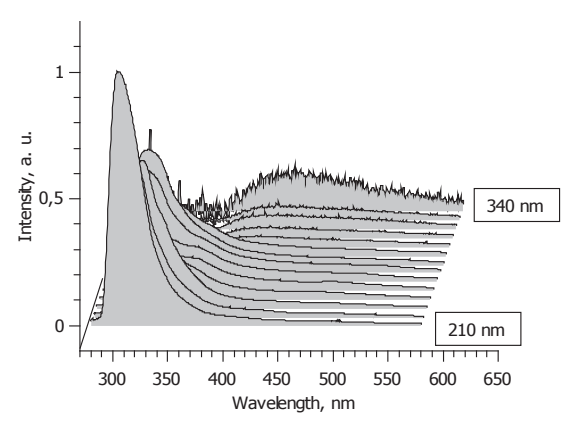


FIGURE 5. The normalized excitation-emission matrix of the scaffold sheet seeded with BHK IR cells

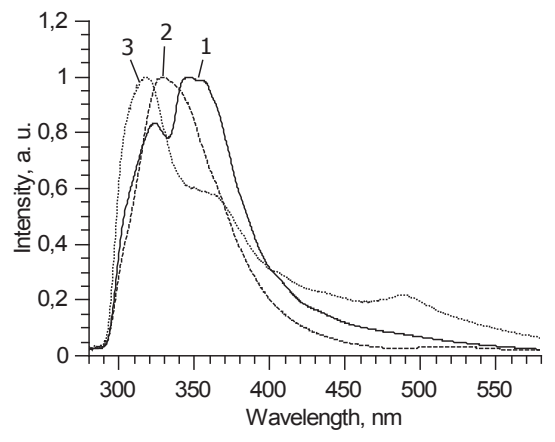


FIGURE 6. Comparison of the fluorescence spectra of the scaffold sheet (1), BHK IR cell suspension (2), and the cell-seeded scaffold sheet (3) for excitation wavelength of 250 nm

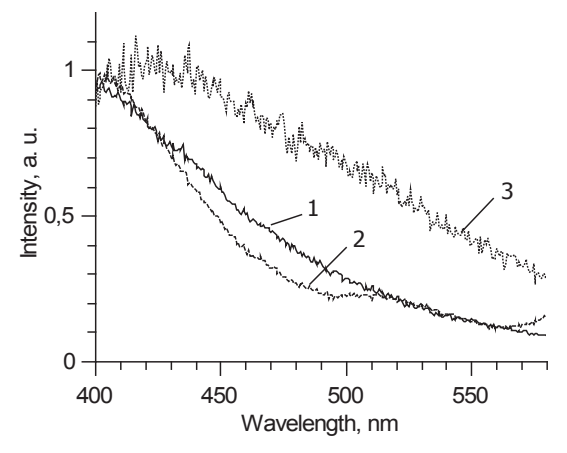


FIGURE 7. Comparison of the fluorescence spectra of the scaffold sheet (1), BHK IR cell suspension (2), and the cell-seeded scaffold sheet (3) for excitation wavelength of 330 nm

REFERENCES

- Y. Z. Lawal, E. S. Garba, M. O. Ogirima, I. L. Dahiru, M. I. Maitama, K. Abubakar, and F. S. Ejagwulu, Ann. Afr. Med. 10, 25–28 (2011).
- 2. I. A. Kirilova, M. A. Sadovoy, and V. T. Podorozhnaja, Spine Surgery J. 3, 72–83 (2012).
- 3. A. Oryan, S. Alidadi, A. Moshiri, and N. Maffulli, J. Orthop. Surg. Res. 9 (2014).
- 4. P. M. Larionov, M. A. Sadovoy, and A. G. Samokhin, Spine Surgery J. 3, 77–85 (2014).
- 5. M. Herrmann, S. Verrier, and M. Alini, Front. Bioeng. Biotechnol. 79 (2015).
- 6. K. H. Neßler, J. R. Henstock, A. J. Haj, et al., J. Theor. Biol. 394, 149–159 (2016).
- 7. Y. Liu, S. H. Teoh, M. S. Chong, et al., Tissue Eng. A 19(7–8), 893–904 (2013).
- 8. Y. Liu and S. H. Teoh, Biotechnol. Adv. 31, 688–705 (2013).
- P. M. Larionov, V. S. Shchukin, A. N. Malov, N. A. Maslov, A. M. Orishich, and A. T. Titov, Appl. Optics 22, 4031–4036 (2000).
- V. M. Fomin, A. M. Karaskov, P. M. Larionov, A. N. Malov, N. A. Maslov, and A. M. Orishich, Dokl. Biolog. Sci. 391(1–6), 296–298 (2003).
- 11. D. V. Subbotin, P. M. Larionov, D. S. Sergeevichev, O. A. Subbotina, G. S. Zaitsev, R. B. Novruzov, A. M. Orishich, A. N. Malov, N. A. Maslov, I. A. Rozhin, E. E. Lushnikova, and L. M. Nepomnyashih, Bullet. Exp. Biol. Med. 148, 684–688 (2009).